

GaPO₄ Sensors for Gravimetric Monitoring during Atomic Layer Deposition at High Temperatures

J. W. Elam^{*,†} and M. J. Pellin[‡]

Energy Systems Division and Materials Science Division, Argonne National Laboratory, Argonne, Illinois 60439

The quartz crystal microbalance is extremely useful for in situ monitoring of thin-film growth by atomic layer deposition (ALD) in a viscous flow environment. Unfortunately, conventional AT-quartz sensors are limited to growth temperatures below ~ 300 °C. Gallium orthophosphate (GaPO₄) is an alternative piezoelectric material offering much greater high-temperature frequency stability than AT-quartz (SiO₂). Our measurements reveal that the temperature coefficient for Y-11° GaPO₄ decreases linearly with temperature reaching 3 Hz/°C at 450 °C. In contrast, the temperature coefficient for the SiO₂ sensor increases as the cube of the sensor temperature to 650 Hz/°C at 390 °C. To examine the effect of temperature fluctuations on the sensor frequency, we exposed the SiO₂ and GaPO₄ sensors to helium pulses at 400 °C. The resulting frequency change measured for the SiO₂ sensor was ~ 40 times greater than that of the GaPO₄ sensor. Next, we performed Al₂O₃ ALD using alternating trimethylaluminum/water exposures at 400 °C and monitored the growth using the SiO₂ and GaPO₄ sensors. The GaPO₄ sensor yielded well-defined pulse shapes in agreement with predictions, while the SiO₂ pulses were severely distorted. Measurements during TiO₂ ALD using alternating titanium tetrachloride/water exposures at 450 °C with the GaPO₄ sensor also showed well-defined ALD mass steps.

Atomic layer deposition (ALD) is a thin-film growth technique that utilizes sequential, self-limiting chemical reactions between gaseous precursors and a solid surface to deposit thin films in a layer-by-layer fashion. Typically, ALD is performed under viscous flow conditions using a pressure of ~ 1 Torr and at temperatures of 100–500 °C, but ALD growth temperatures can reach 900 °C.¹ Moreover, the repeated pulsing of the ALD precursors causes frequent, rapid changes in pressure and deposition rate. These conditions seriously challenge conventional in situ methods for monitoring thin-film growth at the monolayer level. Despite these difficulties, a number of techniques have emerged that perform well during ALD in hot, viscous flow environments including optical reflectivity,² mass spectrometry,³ and quartz crystal microbalance (QCM) methods.⁴

Of these methods, QCM is the most widely used technique for in situ growth monitoring during ALD.^{4–7} The QCM is very useful for determining ALD growth rates, optimizing processing conditions, measuring nucleation phenomena, and elucidating growth mechanisms. The most serious limitation to the QCM technique is that the resonant frequency of typical AT-cut quartz sensors is extremely dependent on temperature.^{8,9} For instance, at 177 °C, the optimal temperature for Al₂O₃ ALD, the AT-cut quartz sensor has a temperature coefficient of ~ 50 Hz/°C so that a temperature increase of only 1 °C causes a frequency increase of 50 Hz and produces an apparent Al₂O₃ thickness change of ~ 18 Å. This change is large compared to the Al₂O₃ ALD growth rate of ~ 1 Å/cycle. Furthermore, the temperature coefficient increases with the cube of the deposition temperature so that temperature-dependent frequency shifts become more severe at higher deposition temperatures. Consequently, slow temperature drift of the ALD reactor as well as rapid temperature fluctuations induced by the ALD reactant vapor pulses render the QCM nearly unusable at temperatures above 300 °C.

Various strategies have been employed to combat this problem. In one method, a reference crystal is positioned near the primary sensor but is isolated from the ALD precursors and the frequency of the reference crystal is subtracted from the primary sensor frequency to compensate for temperature changes.^{6,10} Although this technique corrects for slow thermal drift, temperature transients produced by the ALD precursors are still problematic. In another technique, temperature drift is corrected using baseline subtraction.⁶ This method is just as effective as the reference crystal method, but it suffers from the same inability to compensate for the temperature transients induced by the ALD precursors. It is possible to minimize temperature transients produced by the ALD gases by carefully tuning the temperature profile of the ALD reactor.¹¹ However, temperature changes produced by the enthalpy of the ALD surface reactions cannot be eliminated using this strategy.

- (2) Rosental, A.; Adamson, P.; Gerst, A.; Niiilisk, A. *Appl. Surf. Sci.* **1996**, *107*, 178–183.
- (3) Juppo, M.; Rahtu, A.; Ritala, M.; Leskela, M. *Langmuir* **2000**, *16*, 4034–4039.
- (4) Aarik, J.; Aidla, A.; Kukli, K. *Appl. Surf. Sci.* **1994**, *75*, 180–184.
- (5) Yousfi, E. B.; Fouache, J.; Lincot, D. *Appl. Surf. Sci.* **2000**, *153*, 223–234.
- (6) Rahtu, A.; Ritala, M. *Appl. Phys. Lett.* **2002**, *80*, 521–523.
- (7) Elam, J.; Groner, M.; George, S. *Rev. Sci. Instrum.* **2002**, *73*, 2981–2987.
- (8) Kim, M.-S.; Kim, K.-B. *Han'guk Pusik Hakhoechi* **1997**, *26*, 312–320.
- (9) O'Sullivan, C. K.; Guilbault, G. G. *Biomol. Sens.* **2002**, 291–303.
- (10) Mecea, V. M.; Carlsson, J. O.; Sessler, P.; Bartan, M. *Vacuum* **1995**, *46*, 691–694.
- (11) Rocklein, M. N.; George, S. M. *Anal. Chem.* **2003**, *75*, 4975–4982.

* To whom correspondence should be addressed. E-mail: jlam@anl.gov.

[†] Energy Systems Division.

[‡] Materials Science Division.

(1) Nagasawa, H.; Yamaguchi, Y. *Thin Solid Films* **1993**, *225*, 230–234.

Alternatively, the temperature sensitivity of the quartz mass sensor can be reduced relative to the conventional AT-cut sensors by choosing a different angle of cut. For instance, at 37°30', a zero temperature coefficient is achieved at 250 °C.¹² Unfortunately, the temperature coefficient at this crystal angle changes so rapidly with temperature that the low temperature coefficient is only maintained over a narrow, 20 °C temperature range.¹³ This is inconvenient because it necessitates changing sensor crystals whenever changing deposition temperatures.

Another approach to high-temperature gravimetric monitoring is to choose a piezoelectric material with better temperature-dependent properties. Langisite ($\text{Co}_{0.75}\text{Ni}_{0.25}\text{As}$) and gallium orthophosphate (GaPO_4) have been suggested and demonstrated as alternative piezoelectric materials for resonant mass sensors that are well suited for high-temperature applications.^{14–19} Here we demonstrate that GaPO_4 is well suited for ALD in situ growth monitoring.

The crystal structure of GaPO_4 is homeotypic to quartz (SiO_2)²⁰ where half of the Si atoms, each with four valence electrons, are replaced alternately by Ga and P atoms, with three and five valence electrons, respectively. GaPO_4 mass sensors with a Y-11° cut have a relatively low-temperature coefficient over the full range of typical ALD growth temperatures (100–500 °C). Most importantly, the Y-11° GaPO_4 sensors are ~100 times less sensitive to temperature fluctuations than conventional AT-quartz sensors above 400 °C.^{7,18} In addition, the maximum usable temperature for GaPO_4 is much higher than for quartz. While the SiO_2 piezoelectric constant begins to drop at 300 °C and reaches zero at 573 °C due to a phase transition, the GaPO_4 piezoelectric constant remains nearly constant up to 970 °C.²¹

In this study, Y-11° GaPO_4 sensors obtained from AVL LIST GmbH are compared with conventional AT-quartz sensors for in situ growth monitoring in an ALD flow reactor. In the initial experiments, the temperature coefficients for these two sensors were determined. Next, the effect of the different temperature coefficients on the frequency stability was examined by subjecting the mass sensors to helium gas pulses. Finally, the two sensors were used to monitor the ALD of Al_2O_3 and TiO_2 at temperatures as high as 450 °C.

EXPERIMENTAL SECTION

The experiments were performed using a viscous flow ALD reactor as described elsewhere.⁷ A Maxtek BSH-150 bakeable

sensor head with a maximum operating temperature of ~425 °C held the mass sensor near the center of the reactor flow tube. To prevent deposition on the back surface of the sensor, the sensor housing was continuously purged with ultra-high-purity nitrogen at a mass flow rate of ~20 sccm. Furthermore, the gap between the front surface of the sensor and the Maxtek Cool Drawer crystal holder was filled using a high-temperature conducting epoxy, Epotek P1011. A thermocouple mounted to the bottom of the sensor head monitored the temperature near the mass sensor. To minimize temperature-induced apparent mass changes, the temperature profile of the ALD reactor was adjusted to achieve a uniform temperature distribution around the mass sensor.¹¹ The uniform temperature profile was obtained by adjusting the temperature set points and heater power distribution of four separate temperature-controlled heating zones on the ALD reactor.

Two types of sensor crystals were used in these studies. The first was an AT-cut quartz (SiO_2) sensor with a polished front surface obtained from the Colorado Crystal Corp. (Part CCAT1BK-1007-000). In addition, GaPO_4 sensors with a polished front surface were obtained from AVL LIST GmbH, (Part TXKGAPO00A.A1). These sensors were cut with a Y-11.0° orientation, had a diameter of 14 mm, a resonant frequency of 6 MHz, a flat front surface and a beveled back surface. The Y-11.0° GaPO_4 sensor was selected for this study because it exhibits a relatively low temperature coefficient over the experimentally relevant temperature range for ALD, 100–700 °C.¹⁸ A Maxtek TM400 thickness monitor was used to monitor the SiO_2 or GaPO_4 mass sensor signals and provided a mass resolution of 0.375 ng/cm² with a data update rate of 10 measurements/s.

The Al_2O_3 ALD was performed using alternating exposures to trimethylaluminum (TMA, Aldrich) and deionized water while the TiO_2 ALD used alternating exposures of titanium tetrachloride (TiCl_4 , Aldrich) and deionized water. The chemical precursors were introduced into the reactor using computer-controlled pneumatic diaphragm valves in series with metering valves. The metering valves were adjusted to regulate the precursor flow rate to ~20 sccm and the precursor partial pressure to ~0.1 Torr during the exposures. The ALD timing sequence is specified by t1-t2-t3-t4 where t1 is the exposure time for the first precursor, t2 is the purge time following the first exposure, t3 is the exposure time for the second precursor, and t4 is the purge time following the exposure to the second precursor. The timing sequences used in this study were 1–10–1–10 for Al_2O_3 ALD and 1–5–1–5 for TiO_2 ALD with all times measured in seconds. Viscous flow was maintained using ultra-high-purity nitrogen carrier gas at a pressure of 1 Torr using a mass flow rate of 200 sccm at temperatures of 390–450 °C.

For thin films deposited on a resonant mass sensor, the film thickness, t_F , is given by the Sauerbrey equation:²²

$$t_F = \frac{-(\rho_R c_R)^{1/2}}{2f_R \rho_F} \Delta f_R \quad (1)$$

where ρ_R is the density of the resonator, c_R is the resonator elastic modulus, f_R is the initial (unloaded) frequency of the resonator, ρ_F is the density of the film, and Δf_R is the resonator frequency

- (12) Bechmann, R. *Proc. Inst. Radio Eng.* **1960**, 48, 1494.
- (13) Bechmann, R. *Proc. Inst. Radio Eng.* **1956**, 44, 1600.
- (14) Thanner, H.; Krempel, P. W.; Krispel, F.; Reiter, C.; Selic, R. *Ann. Chim.* **2001**, 26, 161–164.
- (15) Grimshaw, S. F. *Proc. SPIE–Int. Soc. Opt. Eng.* **2004**, 5527, 98–104.
- (16) Seh, H.; Tuller, H.; Fritze, H. *Mater. Res. Soc. Symp. Proc.* **2003**, 756, 175–180.
- (17) Thanner, H.; Krempel, P. W.; Selic, R.; Wallnofer, W.; Worsch, P. M. *J. Therm. Anal. Calorim.* **2003**, 71, 53–59.
- (18) Thanner, H.; Krempel, P. W.; Wallnofer, W.; Worsch, P. M. *Vacuum* **2002**, 67, 687–691.
- (19) Worsch, P. M.; Krempel, P. W.; Wallnofer, W. *Proceedings of IEEE Sensors 2002, IEEE International Conference on Sensors, 1st*, Orlando, FL, United States, June 12–14, 2002; 1st, 589–593.
- (20) Nakae, H.; Kihara, K.; Okuno, M.; Hirano, S. *Z. Kristallogr.* **1995**, 210, 746–753.
- (21) Krispel, F.; Reiter, C.; Neubig, J.; Lenzenhuber, F.; Krempel, P. W.; Wallnofer, W.; Worsch, P. M. *Proceedings of the IEEE International Frequency Control Symposium & PDA Exhibition jointly with the 17th European Frequency and Time Forum*, Tampa, FL, United States, May 4–8, 2003; pp 668–673.

- (22) Sauerbrey, G. *Z. Phys.* **1959**, 155, 206–222.

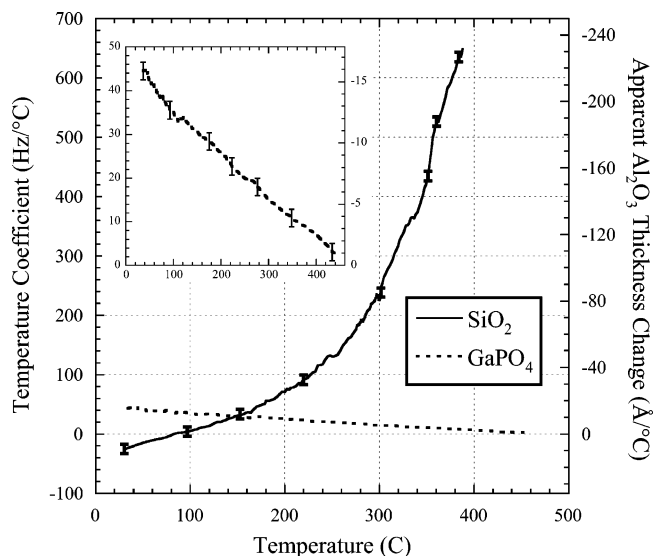


Figure 1. Temperature coefficients for SiO₂ (solid line) and GaPO₄ (dashed line) sensor crystals. Inset shows expanded view of the GaPO₄ data.

change after film deposition. The quantity $(\rho_R c_R)^{1/2}$ is known as the acoustic impedance, Z . For conventional AT-quartz sensors, $\rho_R = 2.648 \text{ g/cm}^3$ and $c_R = 2.947 \times 10^{11} \text{ g/(cm s}^2\text{)}$ so that $Z_{\text{quartz}} = 8.834 \times 10^5 \text{ g/(cm}^2 \text{s)}$, while for Y-11° GaPO₄, $\rho_R = 3.570 \text{ g/cm}^3$ and $c_R = 2.147 \times 10^{11} \text{ g/(cm s}^2\text{)}$ yielding $Z_{\text{GaPO}_4} = 8.755 \times 10^5 \text{ g/(cm}^2 \text{s)}$. Consequently, when using a conventional film thickness monitor that is calibrated for AT-quartz (such as the Maxtek TM400 employed in this study) with the Y-11° GaPO₄ sensor, the resulting thicknesses should be multiplied by $Z_{\text{GaPO}_4}/Z_{\text{quartz}} = 0.991$.

RESULTS AND DISCUSSION

Figure 1 shows the temperature coefficients determined separately for the SiO₂ and GaPO₄ mass sensors. In these measurements, the frequency of the mass sensor was monitored as the sensor temperature was increased slowly at a rate of 3 °C/min from 30 to 450 °C. The left axis in Figure 1 shows the temperature coefficients calculated from the derivative of the frequency versus time measurements, while the right axis plots the apparent Al₂O₃ thickness change by assuming a density of 3.5 g/cm³. The temperature coefficient for SiO₂ increases with the cube of the sensor temperature from -25 Hz/°C at 30 °C to 650 Hz/°C at 393 °C. A 1 °C temperature fluctuation at 393 °C produces an apparent Al₂O₃ thickness change of 230 Å. This change is enormous compared to the ALD Al₂O₃ growth rate of ~1 Å/cycle. Oscillation of the SiO₂ sensor ceased when heated above 393 °C but resumed upon subsequent cooling below 393 °C. In contrast to the SiO₂ sensor results, the temperature coefficient for the GaPO₄ sensor decreases linearly from 43 Hz/°C at 30 °C to 3 Hz/°C at 450 °C. An expanded view of the GaPO₄ measurements is given in the inset to Figure 1. A 1 °C temperature fluctuation at 390 °C will produce an apparent Al₂O₃ thickness change of only 3 Å. Therefore, the GaPO₄ sensor is ~80 times less sensitive to temperature fluctuations than the SiO₂ sensor at 390 °C.

Temperature-induced fluctuations of the mass sensor signal scale with the absolute magnitude of the temperature coefficient.

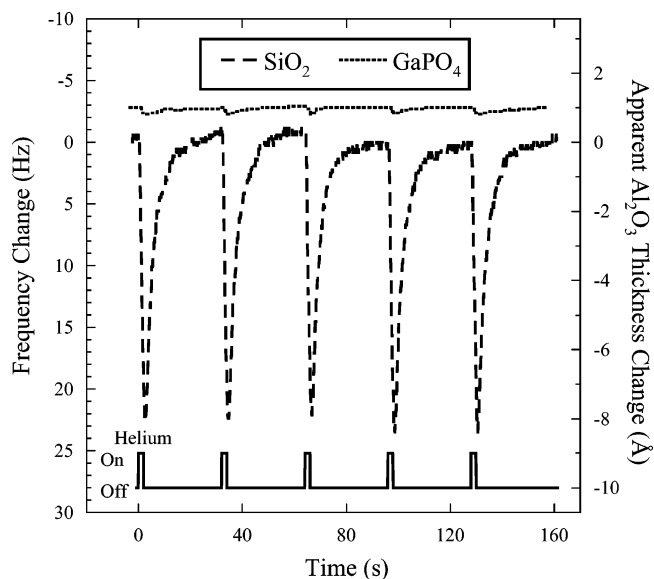


Figure 2. Frequency change induced by helium pulses with a pressure of 1.8 Torr and a duration of 2 s at 390 °C recorded using the SiO₂ (dashed line) and GaPO₄ (dotted line) sensor crystals. The GaPO₄ frequency data has been shifted upward for clarity.

Consequently, GaPO₄ is more sensitive to temperature fluctuations than SiO₂ below 150 °C (Figure 1), suggesting that SiO₂ is more suitable in this temperature range. In our experience, however, temperature effects are tolerable as long as the temperature coefficient remains below ~250 Hz/°C. Because the GaPO₄ temperature coefficient remains below 50 Hz/°C over the full range of examined temperatures from 30 to 450 °C, it is not necessary to switch to an SiO₂ sensor for temperatures below 150 °C.

The much higher temperature coefficient of the SiO₂ sensor compared to the GaPO₄ sensor at 390 °C will dramatically affect the response of the sensor when reactive gas pulses are introduced at higher ALD growth temperatures. These temperature changes occur because the reactive gases do not thermally equilibrate before reaching the sensor and because of the enthalpy of the ALD surface reactions. To examine the effect of thermal disequilibrium, the sensor signals were monitored as helium gas pulses were applied. Helium pulses have been used previously to probe the effects of transient temperature changes on in situ quartz microbalance measurements.¹¹ Helium is an effective probe gas both because of its very high thermal conductivity and because it does not adsorb on the sensor surface. Because helium will not adsorb onto the sensor surface, and because the effects of pressure changes and viscosity loading on the sensor frequency are negligible in these experiments,²³ the observed resonant frequency changes can be attributed solely to changes in the sensor temperature.

Figure 2 shows the frequency response of the SiO₂ (dashed line) and GaPO₄ (dotted line) mass sensors during the application of helium pulses with a duration of 2 s (t₁) and a pressure of 1.8 Torr with 30 s (t₂) purge periods following each helium pulse. The SiO₂ and GaPO₄ sensors were tested in separate experiments using a sensor temperature of 390 °C, a steady-state pressure of

(23) Park, K.; Koh, M.; Yoon, C.; Kim, H.; Kim, H. *J. Supercrit. Fluids* **2004**, *29*, 203–212.

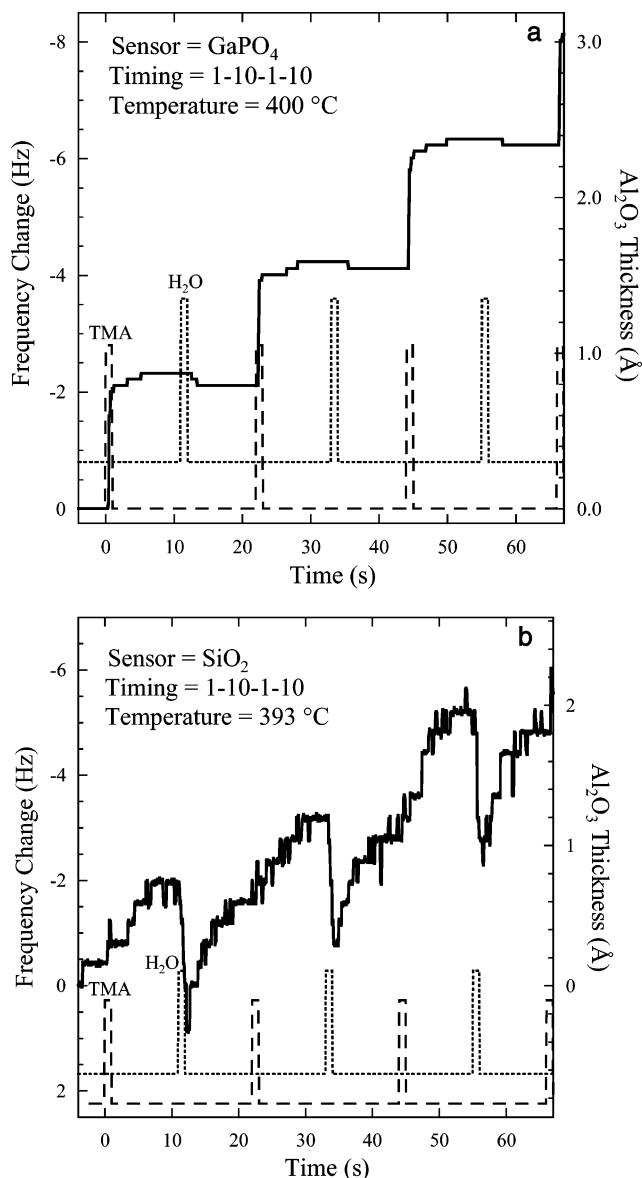


Figure 3. Frequency response recorded during alternating TMA/H₂O exposures for Al₂O₃ ALD using GaPO₄ sensor at 400 °C (a) and SiO₂ sensor at 393 °C (b). The status of the TMA and H₂O dosing valves is indicated by the dashed and dotted lines, respectively.

0.86 Torr, and a nitrogen carrier gas flow of 200 sccm. As shown in Figure 2, the SiO₂ sensor frequency increases by 23 ± 2 Hz as a result of transient heating during each helium pulse. In contrast, the GaPO₄ sensor frequency increases by only 0.53 ± 0.1 Hz during each helium pulse. For comparison, the apparent Al₂O₃ thickness changes corresponding to these frequency changes are indicated by the right-hand axis in Figure 2. The helium pulses produce an apparent Al₂O₃ thickness change of -8.6 ± 0.7 Å on the SiO₂ sensor and only -0.2 ± 0.04 Å on the GaPO₄ sensor.

The relative immunity of the GaPO₄ sensor to temperature-induced frequency transients suggests that the GaPO₄ sensor will perform better than the SiO₂ sensor for ALD measurements at temperatures above ~ 150 °C. Figure 3a shows the response of the GaPO₄ mass sensor during Al₂O₃ ALD at 400 °C using the timing sequence 1-10-1-10. The application of the TMA and H₂O pulses is indicated by the dashed and dotted lines, respectively, at the bottom of the figure. The ALD steps in Figure 3a

show a rapid frequency drop during the TMA exposures followed by a flat region during the TMA purge times. The H₂O exposures produce a small increase in frequency followed by a flat region during the H₂O purges. The thickness changes corresponding to these frequency changes is indicated by the right-hand axis on Figure 3a assuming a density of 3.5 g/cm^3 . These measurements yield a growth rate of 0.67 ± 0.09 Å/cycle that matches well with previous measurements for Al₂O₃ ALD at this temperature.²⁴

The shape of the frequency steps in Figure 3a reflect the Al₂O₃ ALD growth mechanism.²⁵ The step ratio, R , is defined by the net frequency change at the end of purge B (H₂O) divided by the net frequency change at the end of purge A (TMA). This quantity relates to the number of surface hydroxyl groups, n , reacting with each TMA molecule by $R = 51/(72 - 16n)$.²⁵ In Figure 3a, $R = 0.88 \pm 0.10$ so that $n = 0.90 \pm 0.10$. This value matches fairly well with the value $n = 1.2$ measured using in situ mass spectrometry measurements.²⁵

The response of the SiO₂ sensor during Al₂O₃ ALD at 393 °C is given in Figure 3b. The Al₂O₃ ALD steps measured using the SiO₂ sensor are much less defined than the corresponding steps from the GaPO₄ sensor in Figure 3a. In particular, there are no flat regions in Figure 3b during the TMA and H₂O purge periods. Furthermore, the Al₂O₃ ALD steps in Figure 3b show a transient decrease in apparent mass during each H₂O exposure. This feature is very similar to the transient decrease exhibited for the SiO₂ sensor during helium exposures (Figure 2) and probably results from transient heating during the H₂O exposures. Remarkably, the average Al₂O₃ ALD growth rate determined from the SiO₂ sensor is 0.66 ± 0.24 Å/cycle in excellent agreement with the GaPO₄ value of 0.67 ± 0.09 Å/cycle. It is not possible to calculate an ALD step ratio from the data in Figure 3b because there are no flat regions during the purge periods.

If the frequency fluctuations exhibited by the SiO₂ sensor in Figure 3b arise solely from the incomplete thermal equilibration of the ALD gases with the reactor walls, then these fluctuations can be eliminated by carefully tuning the reactor temperature profile.¹¹ However, the enthalpy of the surface chemical reactions may also change the temperature, and hence the frequency, of the SiO₂ sensor. The enthalpy for the reaction between TMA and H₂O is -144 kcal/mol of Al atoms.²⁶ Using the SiO₂ sensor volume and heat capacity, the formation of ~ 1 Al₂O₃ monolayer (10^{15} Al atoms) will heat the sensor by ~ 0.01 °C. From Figure 1, this will cause a frequency change of ~ 6 Hz at 390 °C. This change is comparable to the ~ 2 -Hz transients in Figure 3b so that the reaction enthalpy may explain the frequency transients observed using the SiO₂ sensor. Frequency transients of the SiO₂ sensor caused by reaction enthalpy cannot be eliminated by tuning the reactor temperature profile but are minimized using GaPO₄ sensors.

To explore the high-temperature limit for ALD measurements using the GaPO₄ sensor, we performed TiO₂ ALD at a deposition temperature of 450 °C using alternating TiCl₄/H₂O exposures with the timing sequence 1-5-1-5. Although GaPO₄ mass sensors

(24) Ott, A. W.; Klaus, J. W.; Johnson, J. M.; George, S. M. *Thin Solid Films* **1997**, 292, 135-144.

(25) Rahtu, A.; Alaranta, T.; Ritala, M. *Langmuir* **2001**, 17, 6506-6509.

(26) Weast, R. C.; Astle, M. J., Eds. *CRC Handbook of Chemistry and Physics*; CRC Press: Boca Raton, FL, 1982.

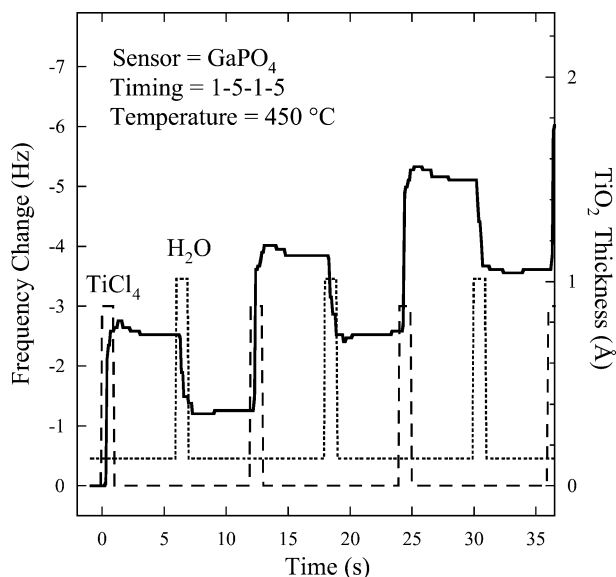


Figure 4. Frequency response recorded during alternating $\text{TiCl}_4/\text{H}_2\text{O}$ exposures for TiO_2 ALD recorded using GaPO_4 sensor at 450°C . The TiCl_4 and H_2O dosing valve status is indicated by the dashed and dotted lines, respectively.

have been used at higher temperatures,¹⁴ 450°C already exceeds the maximum temperature for the BSH-150 sensor head. Figure 4 exhibits a well-defined ALD step structure where the frequency decreases abruptly with each TiCl_4 exposure, increases abruptly with each H_2O exposure, and remains constant during the purge periods. The large frequency increase (mass loss) during each H_2O exposure results from the exchange of the heavy chloride surface species by the lighter hydroxyl surface species. Previous QCM measurements of TiO_2 ALD at 450°C using quartz sensors

required baseline drift compensation and did not yield well-defined steps or flat purge regions.⁶ In Figure 4, the right-hand axis plots the TiO_2 thickness by assuming a density of 4.26 g/cm^3 and yields a growth rate of $0.36 \pm 0.05\text{ Å/cycle}$ in agreement with previous measurements.²⁷

CONCLUSIONS

The quartz crystal microbalance is extremely useful for in situ measurements during the atomic layer deposition of thin films in a viscous flow environment. Unfortunately, microbalance measurements utilizing typical AT-cut quartz sensors are limited to ALD growth temperatures of $<\sim 300^\circ\text{C}$ as a result of the extreme sensitivity of the quartz oscillation frequency to temperature fluctuations. GaPO_4 is a piezoelectric material offering much greater frequency stability at higher temperatures than conventional AT-quartz. We have demonstrated that GaPO_4 sensor crystals yield precise in situ growth measurements during the ALD of Al_2O_3 and TiO_2 films at temperatures as high as 450°C . These measurements are free from the temperature-induced mass transients commonly observed using SiO_2 sensors at higher temperatures. GaPO_4 sensors show great promise to extend the range of allowable in situ ALD measurements to high-temperature processes.

ACKNOWLEDGMENT

This work is supported by the U.S. Department of Energy, BES Materials Sciences, under Contract W-31-109-ENG-38, and by NASA under Work Orders W-19,895 and W-10,091. We are grateful to Peter Worsch and Dietmar Kröger of AVL List GmbH for providing technical support.

Received for review February 25, 2005. Accepted March 29, 2005.

AC050349A

(27) Ritala, M.; Leskela, M.; Nykanen, E.; Soininen, P.; Niinisto, L. *Thin Solid Films* **1993**, 225, 288–295.